



Non-Linear Bending Analysis in Porous FG Circular Rotating Plate with Thermo-Mechanical Loads

Rania M. Tantawy ^{a,*}, Ashraf M. Zenkour ^{b,c}

^a Department of Mathematics, Faculty of Science, Damietta University, P.O. Box 34517, Egypt

^b Department of Mathematics, Faculty of Science, Kafrelsheikh University, Kafrelsheikh 33516, Egypt

^c Department of Mathematics, Faculty of Science, King Abdulaziz University, P.O. Box 80203, Jeddah 21589, Saudi Arabia

Abstract

The current study displays a geometric model of thermo-mechanical symmetric axial bending of a rotating circular porous plate with gradient characteristics and exponential porosity distribution. The thermal and mechanical characteristics of the plate are supposed to be gradient in thickness direction by an exponential porosity distribution law. Using Rissner Mindlin's theory known as first-order deformation theory for small deviation, the equilibrium equations for the bending components are derived. Novelty of the present study is to present the complete thermo-elastic solution of FG porous circular plate to study the resulting bending with distinct boundary conditions. Numerical results for three numerous statuses of boundary conditions are offered and examined to study the effect of the porosity parameter it was found that there is a significant change in the bending components with the variation in the porosity parameter. We conclude from this the importance of geometric models in modern engineering mechanical design.

Keywords: Porosity; Bending, Deflection theory; First order deformation theory; Functionally graded; Circular plate.

1. Introduction

The tremendous progress in industry and the need to produce many composite structures that are produced from materials that are processed to obtain structures characterized by high rigidity and tolerance to greater mechanical forces and less weight. These structures have a wide use in the field of civil, military, and marine engineering in addition to many daily uses in industry. With all this demand in industry, the manufacture of composite structures is very difficult, especially when they consist of several layers with different material properties between the layers. Therefore, there was a need to overcome these problems by producing functionally graded materials to provide better mechanical performance and withstand higher temperatures. During the last three decades, attention has been paid to the manufacture of FGM's and many manufacturing methods have been invented to develop the method of distributing pores in functionally graded materials. Therefore, the current study is concerned with porous composite circular plates, which are one of the most important structures that we encounter daily due to their large presence in the manufacture of machine parts, reciprocating presses, and high-speed ships. In studying the vibration resulting from these structures under the influence of many mechanical forces, the problem of deformation of these plates arises, which is a necessary matter that must be taken into account by designers of composite structures. The research presents a case of deformation of porous composite

* Corresponding author. Rania M. Tantawy, E-mail address: rania_eltantwy@yahoo.com

circular plates obtaining elastic solutions for stresses and strains and calculating displacement is of great importance in the field of structural mechanics. Many researchers and studies presented the problem of deformation in composite structures, including for example, Plaut [1] was interested in studying the thin annular and circular plates for the problem of deformation resulting from large deviations, strains, and rotation using the generalized Reissner theory, and shear distortion neglected. Jing and Duan [2] addressed the buckling of disks with openings using discrete Ritz method (DRM) with certain boundary conditions. Tantawy and Zenkour [3] illustrate the bending analysis of exponential porous rotating viscoelastic FG plates. Yang *et al.* [4] examine bending of 3D mechanical and thermal loads of FG nanocomposite annular and circular disks strengthened with graphene. Vinh *et al.* [5] analysed buckling and bending analysis of porous FG discs by first-order shear deformation notion. Tantawy and Zenkour [6] present the semi-analytical method for porosity influence and hygrothermal effect on FG porous hollow spheres with electric and mechanical forces. Levyakov [7] investigated the buckling analysis in FG circular discs whose material characteristics are graded in z - direction. Tantawy and Zenkour [8] offer thermal effect, magnetic force, rotation, and porosity on FG annular plates with tapered thickness. Najafizadeh and collaborators [9, 10] used first-order shear deformation theory (FSDT) to study buckling of FG circular discs with nonuniform and uniform temperatures. Tantawy and Zenkour [11] investigate porosity distribution (even -uneven) on FG rotating tapered plates with magnetic, electric, thermal, mechanical, and thermal loads. Allam *et al.* [12] discuss the semi-analytical technique for thermoelastic solution for FG annular tapered plate. Ghorashi and Daneshpazhooh [13] calculate the mechanical symmetric load of circular tapered plates. Dai *et al.* [14] introduce a rotating circular steel plate with changeable thickness undergoing thermal and mechanical loading. Khorshidvand *et al.* [15] illustrate a buckling survey of circular FG plates by surface-fixed piezoelectric layers considered first-order shear deformation notion. And many research and scientific studies such as [16-25].

The present goal is to represent a mechanical model of an FG porous rotating circular plate with thickness h . The material characteristic of the plate is graded along z -direction Compatible with to exponential law. A novel collection of equilibrium equations in existence of porosity property, small deflections, and by using first-order shear deformation theory, we get an exact elastic solution for circular porous plate under mechanical and thermal load. Finally, a comparison of the numerical outcomes of bending components for porous and nonporous plates for multiple three-boundary conditions demonstrates the importance of the composite porous structure.

2. Detailing of the mathematical model of a rotating circular plate

The research illustrates a circular rotating functionally graded porous plate with radius a and thickness h axisymmetric about the Z - axis. The circular plate undergoes transversal loads $q_z(r)$, mechanical force and thermal effect $T(Z)$. By using cylindrical coordinates (r, θ, z) , the origin point of the coordinate is similar to the center point of the plate. Mathematical engineering model was designed so that the lower surface is made of PZT-4 and is graded in physical and mechanical properties to the upper surface made of Cadmium Selenide. All physical constants for the two materials are tabulated in Table 1.

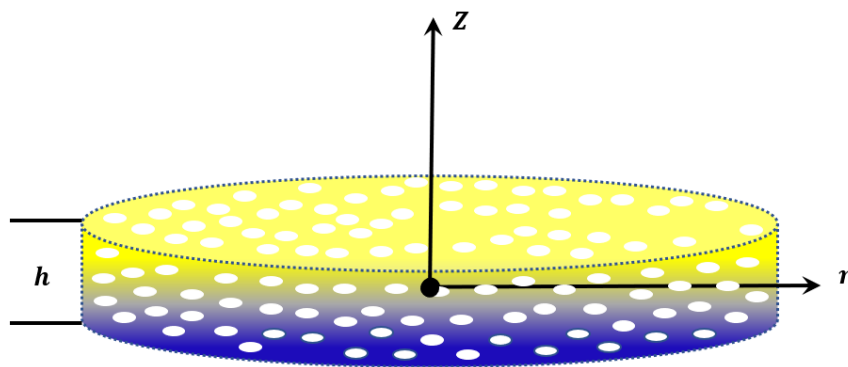


Fig 1: Exponential circular rotating functionally graded porous plate.

Table 1: Thermal and mechanical parameters for plate material

PZT-4 [26]	Cadmium Selenide [27]
$E^{(l)} = 84$ (GPa)	$E^{(u)} = 50$ (GPa)
$\nu^{(l)} = 0.31$	$\nu^{(u)} = 0.35$

$$\begin{array}{ll}
 K_T^{(l)} = 110 \text{ (WK}^{-1}\text{m}^{-1}\text{)} & K_T^{(u)} = 4 \text{ (WK}^{-1}\text{m}^{-1}\text{)} \\
 \alpha_r^{(l)} = 2 \times 10^{-5} \text{ (K}^{-1}\text{)} & \alpha_r^{(u)} = 2.458 \times 10^{-6} \text{ (K}^{-1}\text{)} \\
 \rho^{(l)} = 7500 \text{ (kg m}^{-3}\text{)} & \rho^{(u)} = 5684 \text{ (kg m}^{-3}\text{)}
 \end{array}$$

3. Porosity characteristic of a circular plate

Assume that the porosity properties vary according to an exponential distribution. Previously, the porosity properties were shown using a modulated Mooney-kind exponential equation for porosity as [28, 29]

$$p(z) = p_0 \exp\left(-\frac{\lambda\beta}{1-\beta}\right), \tag{1}$$

where p_0 is the characteristic without pores, λ is the parameter that defines the pores frame, and β ($0 \leq \beta \leq 1$) is the porosity parameter.

Assuming that the thermal and mechanical characteristics of the plate change z-direction of circular porous plate with gradient properties, zenkour [30] has changed the exponential porosity distribution as

$$p(z) = p^{(l)} \exp\left(\mu\left(\frac{z}{h} + \frac{1}{2}\right) - \frac{2\beta}{1-\beta}\right), \tag{2}$$

where $\mu = \ln\left(\frac{p^{(u)}}{p^{(l)}}\right)$, $p^{(l)}$ and $p^{(u)}$ are characteristic of lower and upper surfaces of a circular plate, β is porosity coefficient, and $\beta = 0$ for perfect material (non-porous).

4. Thermal formulation

Assuming that the thermal parameters of the plate change in z-direction according to eq. (2), then the Fourier equation for the temperature in the circular porous plate is [31]

$$-\frac{d}{dz}\left(k(z) \frac{dT(z)}{dz}\right) = 0, \tag{3}$$

with boundary condition

$$T(z)|_{z=-\frac{h}{2}} = T_0, \quad T(z)|_{z=\frac{h}{2}} = T_1, \tag{4}$$

which $k(z)$ is the thermal conductivity coefficient, T_0 and T_1 are temperature at lower and upper surface of porous plate, sequentially.

5. Displacements, stresses, and strains components

The first-order shear deformation theory (FSDT) is often known as Reissner-Mindlin theory and is used to study the deflection produced in a rotating circular porous disk where the transverse shear stress is assumed to be non-zero. Using (FSDT), we find that the displacement components

$$\begin{Bmatrix} u_r(r, z) \\ u_\theta(r, z) \\ u_z(r, z) \end{Bmatrix} = \begin{Bmatrix} u_0(r) \\ 0 \\ w(r) \end{Bmatrix} + z \begin{Bmatrix} \psi(r) \\ 0 \\ 0 \end{Bmatrix} \tag{5}$$

The strain components as a function of displacement using the von-Karmen type are written in the form [27]

$$\begin{Bmatrix} \epsilon_r \\ \epsilon_\theta \\ \gamma_{rz} \end{Bmatrix} = \begin{Bmatrix} \frac{du_0}{dr} + z \frac{d\psi}{dr} + \frac{1}{2} \left(\frac{dw}{dr}\right)^2 \\ \frac{u_0}{r} + z \frac{\psi}{r} \\ \psi + \frac{dw}{dr} \end{Bmatrix} \tag{6}$$

By using Hooke’s law, the stress equations in circular porous plate expressed as

$$\begin{pmatrix} \sigma_r \\ \sigma_\theta \\ \sigma_{rz} \end{pmatrix} = \begin{pmatrix} Q_{11} & Q_{12} & 0 \\ Q_{12} & Q_{22} & 0 \\ 0 & 0 & Q_{66} \end{pmatrix} \begin{pmatrix} \varepsilon_r \\ \varepsilon_\theta \\ \gamma_{rz} \end{pmatrix} - \begin{pmatrix} 1 \\ 1 \\ 0 \end{pmatrix} \frac{E(z)}{1-\nu} \alpha(z) T(z) \tag{7}$$

where $Q_{11} = \frac{E(z)}{1-\nu^2}$, $Q_{12} = \frac{\nu E(z)}{1-\nu^2}$, $Q_{22} = \frac{E(z)}{1-\nu^2}$, $Q_{66} = \frac{E(z)}{2(1+\nu)}$. Suppose that thermal expansion coefficient α and Young's modulus E follow equation (2).

6. Equilibrium relations

The fundamental virtual displacement states, assuming the body is in equilibrium, then virtual work of forces will be zero, consider E_ε is the general strain energy of a circular plate and E_w is general outward work of circular plates. Then, the total energy E terminated as $E \equiv E_\varepsilon - E_w$, were

$$\left. \begin{aligned} E_\varepsilon &= \int_V \sigma_{ij} \varepsilon_{ij} dV = \int_0^a \int_{-\frac{h}{2}}^{\frac{h}{2}} 2\pi (\sigma_r \varepsilon_r + \sigma_\theta \varepsilon_\theta + \sigma_{rz} \gamma_{rz}) r dz dr \\ E_w &= - \int_0^a \int_{-\frac{h}{2}}^{\frac{h}{2}} 2\pi \rho(z) r^2 \omega^2 u_r dz dr - \int_0^a 2\pi r q_z(r) u_z dr \end{aligned} \right\} \tag{8}$$

where $q_z(r)$ is perpendicular pressure on a circular plate radius. From concept of minimum overall energy $\delta E = 0$, then

$$\int_0^a \left\{ \begin{aligned} &\left(N_\theta - \frac{d}{dr}(rN_r) - \rho_1 r^2 \omega^2 \right) \delta u_0 + \left(M_\theta + rQ_r - \frac{d}{dr}(rM_r) - \rho_2 r^2 \omega^2 \right) \delta \psi \\ &- \left(\frac{d}{dr}(rQ_r) + \frac{d}{dr}(rN_r \frac{dw}{dr}) + r q_z \right) \delta w \end{aligned} \right\} dr = 0 \tag{9}$$

where $N_r, N_\theta, M_r, M_\theta, Q_r, \rho_1$ and ρ_2 are postulates as:

$$\left. \begin{aligned} (N_r, N_\theta, Q_r) &= \int_{-\frac{h}{2}}^{\frac{h}{2}} (\sigma_r, \sigma_\theta, \sigma_{rz}) dz \\ (M_r, M_\theta) &= \int_{-\frac{h}{2}}^{\frac{h}{2}} (\sigma_r, \sigma_\theta) z dz \\ (\rho_1, \rho_2) &= \int_{-\frac{h}{2}}^{\frac{h}{2}} \rho(z) (1, z) dz \end{aligned} \right\} \tag{10}$$

where $N_i, (i = r, \theta)$ are stresses, $M_i, (i = r, \theta)$ are moments, and Q_r is the transverse shear for a circular plate per unit length.

From the concept of minimum energy (9), the equilibrium relations are as:

$$\left. \begin{aligned} -\frac{d}{dr}(rN_r) + N_\theta - \rho_1 r^2 \omega^2 &= 0 \\ -\frac{d}{dr}(rM_r) + M_\theta + rQ_r - \rho_2 r^2 \omega^2 &= 0 \\ \frac{d}{dr}(rQ_r) + \frac{d}{dr}(rN_r \frac{dw}{dr}) + r q_z &= 0 \end{aligned} \right\} \tag{11}$$

substituting from Eqs. (7) in Eqs. (10), we deduce that for small deflection

$$\left. \begin{aligned} N_r &= m_{10} \frac{du_0}{dr} + (m_{10} - 2m_{20}) \frac{u_0}{r} + m_{11} \frac{d\psi}{dr} + (m_{11} - 2m_{21}) \frac{\psi}{r} - m_{30} \\ N_\theta &= (m_{10} - 2m_{20}) \frac{du_0}{dr} + m_{10} \frac{u_0}{r} + (m_{11} - 2m_{21}) \frac{d\psi}{dr} + m_{11} \frac{\psi}{r} - m_{30} \\ M_r &= m_{11} \frac{du_0}{dr} + (m_{11} - 2m_{21}) \frac{u_0}{r} + m_{12} \frac{d\psi}{dr} + (m_{12} - 2m_{22}) \frac{\psi}{r} - m_{31} \\ M_\theta &= (m_{11} - 2m_{21}) \frac{du_0}{dr} + m_{11} \frac{u_0}{r} + (m_{12} - 2m_{22}) \frac{d\psi}{dr} + m_{12} \frac{\psi}{r} - m_{31} \end{aligned} \right\} \tag{12}$$

where

$$\begin{aligned}
 m_{1i} &= \int_{-\frac{h}{2}}^{\frac{h}{2}} Q_{11} z^i dz, \quad i = 0,1,2 \\
 m_{2i} &= \int_{-\frac{h}{2}}^{\frac{h}{2}} Q_{66} z^i dz, \quad i = 0,1,2 \\
 m_{3i} &= \int_{-\frac{h}{2}}^{\frac{h}{2}} Q_{22} (1 + \nu) \alpha(z) T(z) z^i dz, \quad i = 0,1
 \end{aligned}$$

Suppose that overall mechanical and thermal coefficients of the porous circular plate obey porosity distribution in Eq. (2). Substituting Eqs. (12) in Eqs. (11), the solution of a differential equation (11) for small deflection in the form [32]

$$\left. \begin{aligned}
 \psi(r) &= \frac{1}{m_{12} \frac{m_{11}^2}{m_{10}}} \left[\left(\frac{1}{2} A_2 - \frac{m_{11}}{2m_{10}} A_1 \right) r - \frac{B(r)}{r} + \frac{\omega^2}{8m_{10}} (m_{11}\rho_1 - m_{10}\rho_2) r^3 \right], \\
 Q_r &= \frac{1}{r} \int r q_z(r) dr, \\
 u_0(r) &= \frac{1}{m_{12} \frac{m_{11}^2}{m_{10}}} \left[\frac{m_{11}}{m_{10}} \frac{B(r)}{r} + \frac{1}{2m_{10}} (A_1 m_{12} - A_2 m_{11}) r - \frac{\omega^2}{8m_{10}} (m_{12}\rho_1 - m_{11}\rho_2) r^3 \right], \\
 w(r) &= \frac{1}{m_{12} \frac{m_{11}^2}{m_{10}}} \left[\left(\frac{1}{4} A_2 - \frac{m_{11}}{4m_{10}} A_1 \right) r^2 + F(r) - \frac{\omega^2}{32m_{10}} (m_{11}\rho_1 - m_{10}\rho_2) r^4 - \frac{Y(r)}{m_{20}k_s} + A_3 \right],
 \end{aligned} \right\} \tag{13}$$

which $Y(r) = \int \frac{1}{r} (\int r q_z(r) dr) dr$, $B(r) = \int r Y(r) dr$, $F(r) = \int \frac{1}{r} B(r) dr$ and k_s is a shear correction parameter. We have three constant unknowns A_1, A_2, A_3 that specified by the boundary conditions of porous plate. After determining unknown constants, we can find displacements and in plate.

7. Bending numerous boundary conditions

The study is concerned with knowing the effect of the bending resulting from a rotating circular plate made of FGM with an exponential porosity distribution. Therefore, three different categories of boundary conditions of plate were taken into consideration [33]

1. Roller-propped circular plate

$$\left. \begin{aligned}
 \text{at } r = 0 \quad & u_0 = 0, \quad \psi = 0, \quad Q_r = 0, \quad \frac{dw}{dr} = 0, \\
 \text{at } r = a \quad & w = 0, \quad N_r = 0, \quad M_r = 0.
 \end{aligned} \right\} \tag{14}$$

2. Hinged circular plate

$$\left. \begin{aligned}
 \text{at } r = 0 \quad & u_0 = 0, \quad \psi = 0, \quad Q_r = 0, \quad \frac{dw}{dr} = 0, \\
 \text{at } r = a \quad & u_0 = 0, \quad w = 0, \quad M_r = 0.
 \end{aligned} \right\} \tag{15}$$

3. Clamped circular plate

$$\left. \begin{aligned}
 \text{at } r = 0 \quad & u_0 = 0, \quad \psi = 0, \quad Q_r = 0, \quad \frac{dw}{dr} = 0, \\
 \text{at } r = a \quad & u_0 = 0, \quad w = 0, \quad \psi = 0, \quad \frac{dw}{dr} = 0.
 \end{aligned} \right\} \tag{16}$$

8. Numerical discussions

In this research, the analytical solution of a circular rotating elastic plate made of a FG with properties that are graded in z-direction is presented. The plate is undergoing an exponential porosity distribution. Plate is also subjected to thermal influence and mechanical forces. To study the numerical results of the plate, we assume that lower surface of plate is made of PZT-4 and has properties that are graded in z- direction until upper surface is made of CdSe material. Numerical results are illustrated and discussed for three several

collections of boundary conditions with proposal of dimensionless variables in the form

$$\left. \begin{aligned} \bar{z} &= \frac{z}{h}, & \bar{r} &= \frac{r}{a}, & \bar{T}(\bar{z}) &= \frac{T(\bar{z})}{T_0}, \\ \bar{N}_r &= \frac{N_r}{\rho^{(l)} \omega^2 a^2 10^3}, & \bar{M}_r &= \frac{M_r}{\pi a^2 q_z 10^7}, & \bar{\sigma}_r &= \frac{\sigma_r}{\rho^{(l)} \omega^2 a^3 10^2}, \\ \bar{p}(\bar{z}) &= \frac{p(\bar{z})}{p^{(l)}} = \exp \left[\mu \left(\bar{z} + \frac{1}{2} \right) - \frac{2\beta}{1-\beta} \right], \end{aligned} \right\}$$

and assuming some numerical constants

$$\left. \begin{aligned} \omega &= 1000 \text{ rad sec}^{-1}, & q_z &= 0.014 \text{ Gpa}, & z &= 0.25, \\ T_0 &= 298 \text{ K}, & T_1 &= 373 \text{ K}. \end{aligned} \right\}$$

8.1. Roller-propped circular plate

Figure 2 shows the bending components of bending forces \bar{N}_r , moments \bar{M}_r , radial stresses $\bar{\sigma}_r$ and displacements \bar{u}_r , \bar{w} of a roller-propped circular porous plate in the radial direction with variation in porosity parameter $\beta = 0.1, 0.3, 0.5, 0.7$ and a non-porous plate $\beta = 0$. Figure 2a is value of force \bar{N}_r with changing porosity coefficient β . It is clear from the figure that force \bar{N}_r obeys boundary conditions on circular porous plate. It is obvious that there is an inverse relation among porosity coefficient β and force \bar{N}_r , as value of force \bar{N}_r decreases with increasing porosity coefficient β . The high-level value of force \bar{N}_r is accomplished in a non-porous plate $\beta = 0$ and the lowly value of force \bar{N}_r is done at $\beta = 0.7$. As for the Figure 2b, it shows the value of the moments \bar{M}_r on the rotating porous circular plate with variation in porosity parameter β . Figure shows a direct relationship between the moments \bar{M}_r and the porosity coefficient β , which highest value of moments \bar{M}_r is done at $\beta = 0.7$ and lowest value of moments \bar{M}_r is expressed in status of non-porous plate $\beta = 0$. Figure 2b acquires boundary conditions of the plate, where $\bar{M}_r = 0$ vanishes at the outer radius $\bar{r} = 1$. The radial stress $\bar{\sigma}_r$ curves of the porous plate with several values of porosity coefficient β are seen in Fig. 2c. The results of radial stress $\bar{\sigma}_r$ curves agree with the results of the forces \bar{N}_r with various porosity coefficients β . The figure shows an inverse relationship between the radial stress $\bar{\sigma}_r$ and the porosity coefficient β , where high-rise value of radial stress $\bar{\sigma}_r$ is status of non-porous plate $\beta = 0$ and lowest value of radial stress $\bar{\sigma}_r$ at $\beta = 0.7$. Figure 2d is displacement value \bar{u}_r in radius direction \bar{r} with variation in porosity coefficient β . The figure shows an inverse relationship between displacement \bar{u}_r and porosity coefficient β . It is evident that high-level displacement value \bar{u}_r is done in non-porous plate $\beta = 0$ and highest displacement value \bar{u}_r is achieved in $\beta = 0.7$. Figure 2e illustrates the displacement value \bar{w} in the circular porous plate. From the figure, the displacement \bar{w} satisfies the boundary conditions and vanishes $\bar{w} = 0$ at the outer radius $\bar{r} = 1$ of the plate. It is also evident that there is a direct relation among displacement \bar{w} and porosity coefficient β , achieving highest displacement value \bar{w} when $\beta = 0.7$, while the lowest displacement value is in non-porous plate $\beta = 0$.

8.2. Hinged circular plate

The bending components \bar{N}_r , \bar{M}_r , radial stress $\bar{\sigma}_r$ and displacement \bar{u}_r , \bar{w} of the plate in Fig. 3 are studied with the change of porosity parameter β in porous and non-porous plate. Figure 3a discusses the force \bar{N}_r curves of the Hinged circular plate with the change of porosity coefficient β . The lowest value of force \bar{N}_r is done in non-porous plate $\beta = 0$. Figure 3b presents the moment values \bar{M}_r with the rotating circular porous plate satisfying the boundary conditions, i.e., $\bar{M}_r = 0$ at $\bar{r} = 1$. The figure displays a direct relationship between the moments \bar{M}_r and porosity coefficient β , where high-level moment value \bar{M}_r is done at $\beta = 0.7$, while the lowest moment value \bar{M}_r is done in non-porous plate $\beta = 0$. As for the Fig. 3c, it shows the radial stress $\bar{\sigma}_r$ with the change in the porosity coefficient β . It is evident that radial stress $\bar{\sigma}_r$ curves join same behavior as force curves \bar{N}_r . It is clear from Fig. 3c that lowest value of radial stress $\bar{\sigma}_r$ is done in non-porous plate $\beta = 0$. Figure 3d displays displacement value \bar{u}_r with different values of the porosity coefficient β . The figure shows a direct relationship between the porosity coefficient β and the displacement \bar{u}_r . Higher value of porosity coefficient β , higher displacement value \bar{u}_r , achieving highest displacement value \bar{u}_r at $\beta = 0.7$. Figure 3e presents displacement value \bar{w} in radius direction \bar{r} , where displacement value \bar{w} vanishes at external radius $\bar{r} = 1$, satisfying boundary conditions of porous plate. Behavior of displacement curves \bar{w} agrees with moment curves \bar{M}_r , where the highest displacement value \bar{w} is achieved at $\beta = 0.7$ and the lowest displacement value \bar{w} is acquired in status of non-porous plate $\beta = 0$.

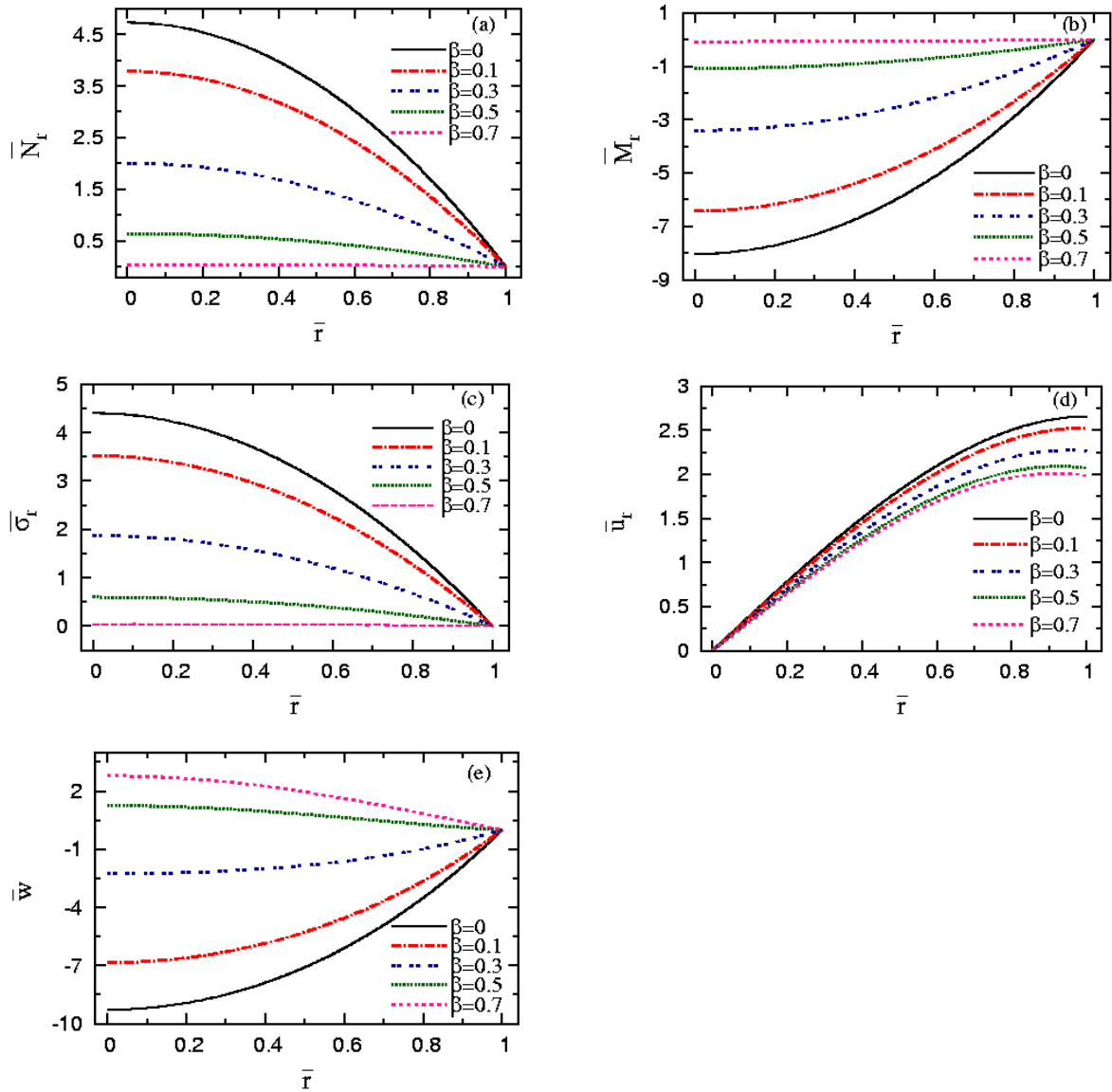


Fig 2: Forces, moments, radial stress, and displacement for roller-propped circular porous plates with numerous porosity parameters.

8.3. Hinged circular plate

In a clamped circular plate, the bending and displacement components with the gradient of the porosity coefficient β are presented in Fig. 4. Figure 4a offers value of force \bar{N}_r with multiple values of porosity coefficient β . It is clear that the force \bar{N}_r curves reduce in direction of increasing radius \bar{r} . Value of forces \bar{N}_r also achieves its lowest value in non-porous plate $\beta = 0$. As for value of moments \bar{M}_r in rotating porous disk, it is presented in Fig. 4b and it is evident that there is a reverse relation among moments \bar{M}_r and porosity coefficient β , where high-level value of moments \bar{M}_r is acquired in non-porous plate $\beta = 0$, while lowest value of moments \bar{M}_r is done at $\beta = 0.7$. Value of radial stress $\bar{\sigma}_r$ is shown in Fig. 4c. Radial stress curves $\bar{\sigma}_r$ intersect with change in porosity coefficient β when $\bar{r} \cong 0.46$. Radial stress curves $\bar{\sigma}_r$ also decrease in radius direction \bar{r} outward. It is evident from Fig. 4d that displacement curves \bar{u}_r are consistent with several values of porosity coefficient β . It is offered that displacement value $\bar{u}_r = 0$ at center of rotating circular plate $\bar{r} = 0$, and at the outer radius $\bar{r} = 1$. The displacement value \bar{u}_r increases from center of plate to outer radius of plate. In Fig. 4e,

the displacement value \bar{w} is displayed at multiple values of porosity parameter β . Curves decrease from center of plate $\bar{r} = 0$ to outer radius $\bar{r} = 1$ of the plate. It is evident that displacement curves \bar{w} are consistent with change in porosity parameter β .

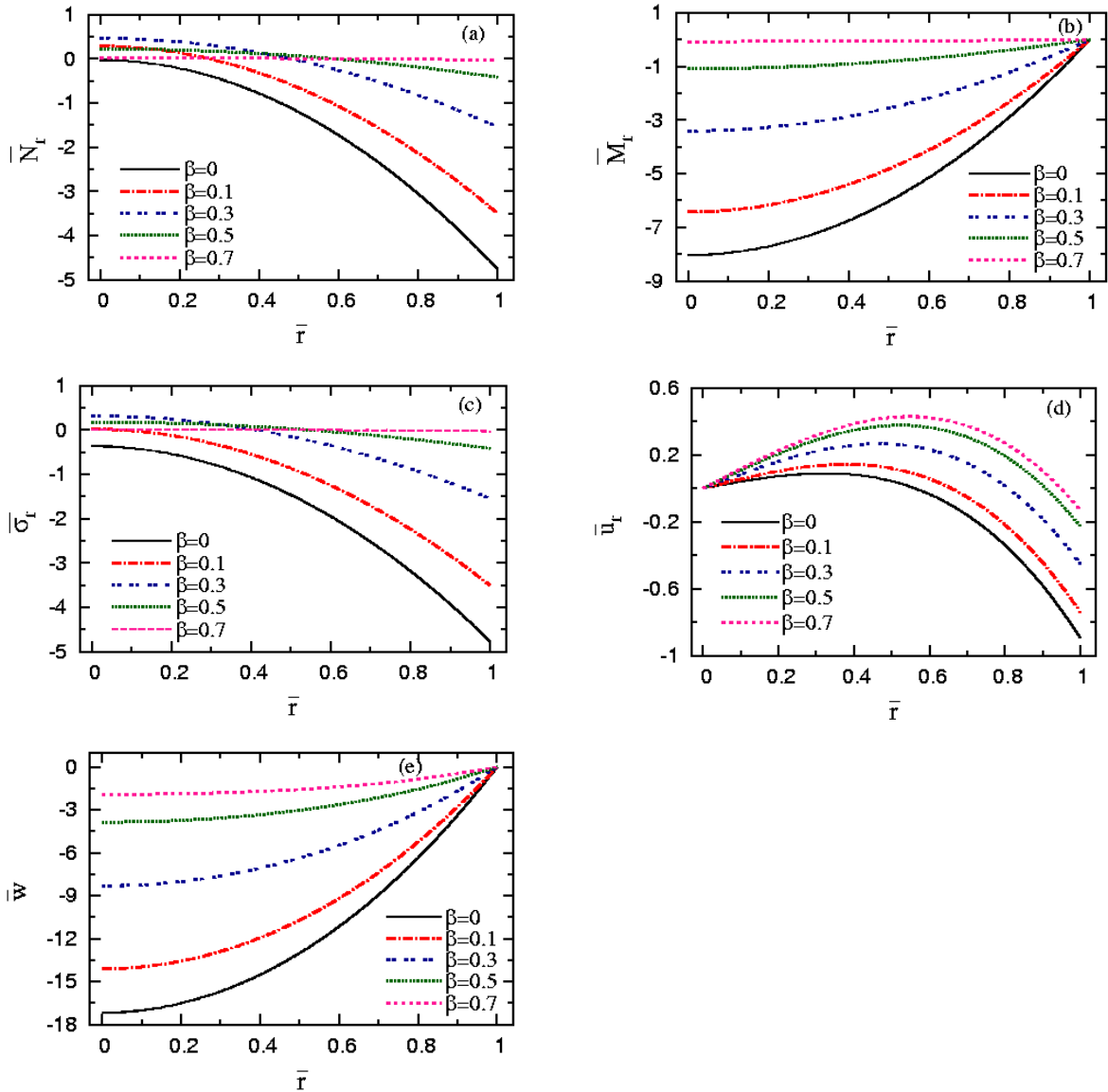


Fig 3: Forces, moments, radial stress and displacement for hinged circular porous plates with numerous porosity parameters.

9. Conclusion

In results, the investigation of FG porous circular rotating plate appears significant insights into those non-linear bending analysis and activity under different boundary conditions as well as the influence of temperature and matter characteristics are graded in thickness of porous plate. Target is to present the bending on the circular plate with porosity distribution. The results summarized as follows

- FSDT yields an exact solution for bending components and displacement.
- Numerical comes for various values of porosity coefficient of graded porous circular plate material with

varying boundary conditions were compared and the results showed significant differences in the results.

- In the status of roller-roller-propped circular plate, the results showed that in non-porous plate, lowest values of moments and value and the highest values of stress resultant and radial stress were achieved.
- In the status of hinged circular plate, highest value of bending components, radial stress, and displacement is done in a non-porous disc.
- In the status of clamped circular plate, the value of bending and displacement components varies with the porosity coefficient and the radius value.
- Developing geometric models of porous circular discs with gradient properties is very important for stress management and energy efficiency enhancement.

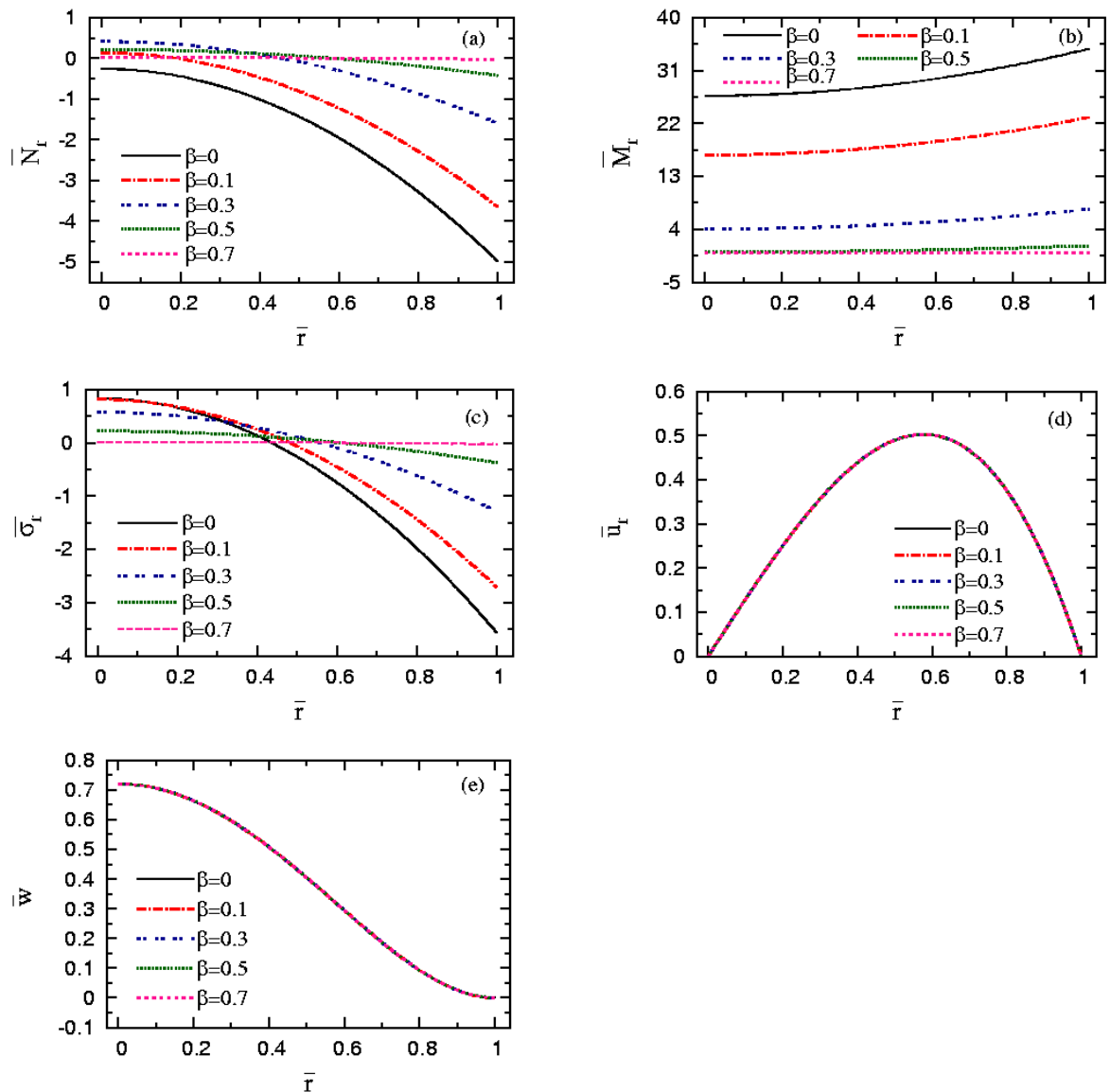


Fig 4: Forces, moments, radial stress, and displacement for clamped circular porous plates with numerous porosity parameters.

References

- [1] R. H. Plaut, Generalized Reissner analysis of large axisymmetric deflections of thin circular and annular plates, *International Journal of Solids and Structures*, Vol. 203, pp. 131-137, 2020.
- [2] Z. Jing, L. Duan, Discrete Ritz method for buckling analysis of arbitrarily shaped plates with arbitrary cutouts, *Thin-Walled Structures*, Vol. 193, pp. 111294, 2023.
- [3] R. M. Tantawy, A. M. Zenkour, Bending Response of a Rotating Viscoelastic Functionally Graded Porous Disk with Variable Thickness, *Journal of Computational Applied Mechanics*, Vol. 54, No. 4, pp. 482-500, 2023.
- [4] B. Yang, S. Kitipornchai, Y.-F. Yang, J. Yang, 3D thermo-mechanical bending solution of functionally graded graphene reinforced circular and annular plates, *Applied Mathematical Modelling*, Vol. 49, pp. 69-86, 2017.
- [5] P. Van Vinh, N. Van Chinh, A. Tounsi, Static bending and buckling analysis of bi-directional functionally graded porous plates using an improved first-order shear deformation theory and FEM, *European Journal of Mechanics-A/Solids*, Vol. 96, pp. 104743, 2022.
- [6] R. Tantawy, A. M. Zenkour, Effect of Porosity and Hygrothermal Environment on FGP Hollow Spheres under Electromechanical Loads, *Journal of Applied and Computational Mechanics*, Vol. 8, No. 2, pp. 710-722, 2022.
- [7] S. Levyakov, Wrinkling of pressurized circular functionally graded plates under thermal loading, *Thin-Walled Structures*, Vol. 137, pp. 284-294, 2019.
- [8] R. Tantawy, A. Zenkour, Effects of Porosity, Rotation, Thermomagnetic, and Thickness Variation on Functionally Graded Tapered Annular Disks, *Information Sciences Letters*, Vol. 12, No. 3, pp. 1133-1150 2023.
- [9] M. Najafizadeh, M. Eslami, First-order-theory-based thermoelastic stability of functionally graded material circular plates, *AIAA journal*, Vol. 40, No. 7, pp. 1444-1450, 2002.
- [10] M. Najafizadeh, B. Hedayati, Refined theory for thermoelastic stability of functionally graded circular plates, *Journal of thermal stresses*, Vol. 27, No. 9, pp. 857-880, 2004.
- [11] R. Tantawy, A. M. Zenkour, Even and Uneven Porosities on Rotating Functionally Graded Variable-thickness Annular Disks with Magneto-electro-thermo- mechanical Loadings, *Journal of Applied and Computational Mechanics*, Vol. 9, No. 3, pp. 695-711, 2023.
- [12] M. N. Allam, R. Tantawy, A. M. Zenkour, Thermoelastic stresses in functionally graded rotating annular disks with variable thickness, *Journal of Theoretical and Applied Mechanics*, Vol. 56, No. 4, pp. 1029-1041, 2018.
- [13] M. Ghorashi, M. Daneshpazhooh, Limit analysis of variable thickness circular plates, *Computers & Structures*, Vol. 79, No. 4, pp. 461-468, 2001.
- [14] H.-L. Dai, T. Dai, X. Yan, Thermoelastic analysis for rotating circular HSLA steel plates with variable thickness, *Applied Mathematics and Computation*, Vol. 268, pp. 1095-1109, 2015.
- [15] A. R. Khorshidvand, M. Jabbari, M. Eslami, Thermo-electro-mechanical buckling of shear deformable hybrid circular functionally graded material plates, *Mechanics of Advanced Materials and Structures*, Vol. 22, No. 7, pp. 578-590, 2015.
- [16] S. E. Alavi, M. M. Shirbani, A. M. Hassani, Analytical investigation of the effect of temperature difference between layers of unimorph piezoelectric harvesters, *Iranian Journal of Science and Technology, Transactions of Mechanical Engineering*, Vol. 48, No. 1, pp. 293-306, 2024.
- [17] M. Bayat, B. Sahari, M. Saleem, A. Hamouda, J. Reddy, Thermo elastic analysis of functionally graded rotating disks with temperature-dependent material properties: uniform and variable thickness, *International Journal of Mechanics and Materials in Design*, Vol. 5, pp. 263-279, 2009.
- [18] Y.-L. Chung, Z.-X. Ou, Exact bending solutions of circular sandwich plates with functionally graded material-undercoated layer subjected to axisymmetric distributed loads, *Journal of Sandwich Structures & Materials*, Vol. 23, No. 7, pp. 2856-2881, 2021.
- [19] D. Gayen, Thermo-elastic buckling and free vibration behavior of functionally graded beams with various materials gradation laws, *International Journal on Interactive Design and Manufacturing (IJIDeM)*, pp. 1-20, 2024.
- [20] H. Guo, X. Zhuang, T. Rabczuk, A deep collocation method for the bending analysis of Kirchhoff plate, *arXiv preprint arXiv:2102.02617*, 2021.
- [21] Z. Jing, L. Duan, S. Wang, Buckling optimization of variable-stiffness composite plates with two circular holes using discrete Ritz method and potential flow, *International Journal of Solids and Structures*, Vol. 297, pp. 112845, 2024.

- [22] Y. Li, Y. Li, Q. Qin, L. Yang, L. Zhang, Y. Gao, Axisymmetric bending analysis of functionally graded one-dimensional hexagonal piezoelectric quasi-crystal circular plate, *Proceedings of the Royal Society A*, Vol. 476, No. 2241, pp. 20200301, 2020.
- [23] R. M. Tantawy, A. M. Zenkour, Logarithmic and trigonometric porosity distributions in rotating functionally graded viscoelastic tapered disk, *Mechanics Based Design of Structures and Machines*, pp. 1-30, 2025.
- [24] Z.-x. Yang, X.-t. He, X. Li, Y.-s. Lian, J.-y. Sun, An electroelastic solution for functionally graded piezoelectric circular plates under the action of combined mechanical loads, *Materials*, Vol. 11, No. 7, pp. 1168, 2018.
- [25] A. M. Zenkour, R. M. Tantawy, Rotating Exponentially Graded Variable-thickness Annular Piezoelectric Porous Disks, *Journal of Vibration Engineering & Technologies*, Vol. 13, No. 2, pp. 166, 2025.
- [26] Y. Ootao, Y. Tanigawa, Transient piezothermoelastic analysis for a functionally graded thermopiezoelectric hollow sphere, *Composite Structures*, Vol. 81, No. 4, pp. 540-549, 2007/12/01/, 2007.
- [27] A. G. Arani, R. Kolahchi, A. M. Barzoki, A. Loghman, Electro-thermo-mechanical behaviors of FGPM spheres using analytical method and ANSYS software, *Applied Mathematical Modelling*, Vol. 36, No. 1, pp. 139-157, 2012.
- [28] W. Pabst, E. Gregorova, Effective elastic properties of alumina-zirconia composite ceramics-Part 2. Micromechanical modeling, *Ceramics- Silikaty*, Vol. 48, No. 1, pp. 14-23, 2004.
- [29] W. Pabst, E. Gregorova, G. Ticha, E. Tynova, Effective elastic properties of alumina-zirconia composite ceramics- part 4. Tensile modulus of porous alumina and zirconia, *Ceramics- Silikaty*, Vol. 48, No. 4, pp. 165-174, 2004.
- [30] A. M. Zenkour, A quasi-3D refined theory for functionally graded single-layered and sandwich plates with porosities, *Composite Structures*, Vol. 201, pp. 38-48, 2018.
- [31] G. Paria, Magneto-elasticity and magneto-thermo-elasticity, *Advances in applied mechanics*, Vol. 10, pp. 73-112, 1966.
- [32] M. Bayat, M. Saleem, B. B. Sahari, A. Hamouda, E. Mahdi, Thermo elastic analysis of a functionally graded rotating disk with small and large deflections, *Thin-Walled Structures*, Vol. 45, No. 7-8, pp. 677-691, 2007.
- [33] J. Reddy, C. Wang, S. Kitipornchai, Axisymmetric bending of functionally graded circular and annular plates, *European Journal of Mechanics-A/Solids*, Vol. 18, No. 2, pp. 185-199, 1999.